Downregulation of TRPC6 regulates ERK1/2 to prevent sublytic C5b-9 complement complex-induced podocyte injury through activating autophagy

YUANYUAN LI, YOUFU FANG and JING LIU

Department of Pediatrics, Weifang Yidu Central Hospital, Weifang, Shandong 262550, P.R. China

Abstract. Idiopathic membranous nephropathy (IMN) is a common glomerular disease, in which 50-60% of patients can progress to end-stage renal disease within 10-20 years, seriously endangering human health. Podocyte injury is the direct cause of IMN. Sublytic C5b-9 complement complex induces damage in podocytes' structure and function. In sublytic C5b-9 treated podocytes, the expression of canonical transient receptor potential 6 (TRPC6) is increased. However, the specific mechanism of TRPC6 in sublytic C5b-9 treated podocytes is unclear. The present study aimed to reveal the effect and mechanism of TRPC6 on sublytic C5b-9-induced podocytes. Normal human serum was stimulated using zymosan to form C5b-9. A lactate dehydrogenase release assay was used to examine C5b-9 cytotoxicity in podocytes. The RNA and protein expression levels were analyzed using reverse transcription-quantitative PCR, western blotting and immunofluorescent assay, respectively. Cell Counting Kit-8 assay and flow cytometry were carried out to test the viability and apoptosis of podocytes, respectively. Transmission electron microscopy was used to observe autophagic vacuole. F-actin was tested through phalloidin staining. Sublytic C5b-9 was deposited and TRPC6 expression was boosted in podocytes stimulated through zymosan activation serum. Knockdown of TRPC6 raised the viability and reduced the apoptosis rate of sublytic C5b-9-induced podocytes. Meanwhile, transfection of small-interfering (si)TRPC6 facilitated autophagy progression and enhanced the activation of cathepsin B/L

in sublytic C5b-9-induced podocytes. The phosphorylation level of ERK1/2 was receded in siTRPC6 and sublytic C5b-9 co-treated podocytes. Moreover, the addition of the ERK1/2 activator partially reversed the effect of TRPC6 inhibition on sublytic C5b-9-induced podocytes. TRPC6 knockdown reduced the damage of sublytic C5b-9 to podocytes by weakening the ERK1/2 phosphorylation level to activate autophagy. These results indicated that targeting TRPC6 reduced the injury of sublytic C5b-9 on podocytes.

Introduction

Membranous nephropathy (MN) is a glomerular disease characterized by glomerular basement membrane thickening, podocyte injury and proteinuria (1,2). MN is divided into idiopathic MN (IMN) and secondary MN (1). IMN is one of the most common pathological types, which is an autoimmune disease (3). The pathogenesis is that antibodies bind to receptor-associated proteins on the surface of glomerular podocytes, forming subepithelial *in situ* immune complexes to activate complement and form the attacking membrane complex C5b-9 (3). The effect of sublytic C5b-9 on podocytes leads to changes in podocytes such as fusion of podocytes processes, apoptosis and abscission from the glomerular basement membrane, resulting in structural and functional dysfunction of glomerular filtration barrier and ultimately proteinuria (4). The podocyte is the epithelial cell of the renal follicle and terminally differentiated cell. The destruction of podocyte integrity and the reduction of podocyte numbers serve an important role in the course of membranous nephropathy (5). The therapy of IMN mainly relies on immune suppression, but the effects are not satisfactory. Therefore, to find a more effective treatment for IMN, it is very important to study the molecular mechanism of podocyte injury.

The complement system is a set of precisely regulated protein reaction systems, including >30 soluble proteins and membrane-bound proteins, which exist widely in serum, tissue fluid and cell membrane surface (6). Most of the complement components exist in the form of non-active enzyme precursors, which show various biological activities when activated by active substances (7). Depending on cell membrane properties and surface inhibitors, the assembly of C5b-9 on cell membranes has certain biological effects. When assembling on the non-nucleated cell membrane such as that of a red

Correspondence to: Mr. Youfu Fang, Department of Pediatrics, Weifang Yidu Central Hospital, 5168 Jiangjunshan Road, Qingzhou, Weifang, Shandong 262550, P.R. China
E-mail: fangyoufu2020@163.com

Abbreviations: IMN, idiopathic membranous nephropathy; TRPC6, transient receptor potential 6; MN, membranous nephropathy; PHN, passive Heymann nephritis; TRP, transient receptor potential; NHS, normal human serum; ZAS, zymosan activated serum; LDH, lactate dehydrogenase; SDS-PAGE, SDS-polyacrylamide gel electrophoresis; PVDF, polyvinylidene difluoride

Key words: TRPC6, C5b-9, podocyte, autophagy, ERK1/2

blood cell, C5b-9 forms transmembrane channels to dissolve the cell. In the surface assembly of nucleated cells, due to the presence of limiting factors, C5b-9 shallowly inserts into the membrane and cannot cause membrane perforation and rupture, which is called sublytic C5b-9 (8,9). Sublytic C5b-9 activates intracellular signaling pathways, prompting cells to release inflammatory factors and cytokines, leading to cell apoptosis, necrosis, cytolysis, stress response and proliferation (9). Complement activation is one of the most important mechanisms in the occurrence and development of glomerular diseases (10,11). For instance, the end product of complement activation sublytic C5b-9-induced immune injury of the renal tubular by regulating the expression level of NLRP3 (12). Sublytic C5b-9 could induce podocyte injury and proteinuria in passive Heymann nephritis (PHN) rats (13).

Autophagy is a biological process in which cytoplasmic macromolecules and organelles degrade in membrane vesicles. Podocytes maintain autophagy in some measure to maintain their normal physiological functions (14). The autophagy activity of podocytes is much higher than that of other mammalian cells, suggesting that podocytes are essential for podocyte function. A previous study showed that inhibition of autophagy leads to severe podocyte damage and albuminuria production (15). *In vitro* studies showed that C5b-9 could block the fusion of autophagy lysosomes podocyte, thus causing podocyte apoptosis and promoting IMN development (16). Therefore, improving the autophagy activity of podocytes may be a potential treatment method for IMN.

Transient receptor potential (TRP) family protein mutation causes a variety of kidney diseases such as hypocalcemia and polycystic kidney disease (17). The canonical transient receptor potential 6 (TRPC6) belongs to the TRP superfamily of ion channel-forming proteins. TRPC6 is a component of the slit diaphragm and plays an important role in regulating renal function (18,19). Changes in the expression level of TRPC6 and channel function lead to calcium influx leading to the development of glomerular diseases (19). Moller *et al* (20), found that TRPC6 expression was increased in the glomerulus of PHN rats. The research found that dexamethasone can resist podocyte injury by stabilizing TRPC6 expression (21). Furthermore, TRPC6 was reported to serve an important role in cell autophagy. For example, the knockdown of TRPC6 can enhance the autophagy of tubular epithelial cells and thus play a protective role on the cells in renal ischemia-reperfusion injury (18). In angiotensin II-induced podocyte apoptosis, TRPC6 knockout can relieve the inhibition of autophagy and play a protective role in podocytes (22). Researchers found that increased phosphorylation levels of ERK were detected in sublytic C5b-9-induced podocytes (23). Moreover, activating ERK1/2 could block the autophagy of podocytes in diabetic nephropathy (24). TRPC6 increased intracellular Ca^{2+} phosphorylated ERK1/2 to activate ERK1/2 in renal ischemia/reperfusion (18). Furthermore, a previous study reported that the expression of TRPC6 was elevated in the podocyte induced by C5b-9 (20). However, the mechanism of TRPC6 in C5b-9-induced podocytes needs to be further studied.

The present study established a sublytic C5b-9-induced podocyte injury cell model, detected the effect of TRPC6 on sublytic C5b-9-induced podocyte injury and verified whether TRPC6 regulated sublytic C5b-9-mediated inhibition of autophagy in the podocytes.

Materials and methods

Podocyte culture and establishment of injury model. Mouse podocyte cell line MPC5 immortalized through simian virus 40 treatment was purchased from the Cell Bank of the Chinese Academic of Sciences (Shanghai, China). Cells were cultured in RPMI 1640 medium (Gibco; Thermo Fisher Scientific, Inc.) supplied with 10% fetal bovine serum (FBS; Gibco; Thermo Fisher Scientific, Inc.) containing 100 U/ml penicillin-streptomycin and 10 U/ml of mouse recombinant γ-interferon (R&D Systems, Inc.). To maintain epithelial phenotype, $5x10^6$ cells were cultured in a humidified atmosphere with 95% air and 5% CO_2 at 33˚C. When reaching 70% confluence, cells were maintained for 10-14 days on a plate coated with type I collagen (Gibco; Thermo Fisher Scientific, Inc.) without γ-interferon at 37˚C for differentiation (23). The fully differentiated cells stopped growing and arborized cells were kept, which were used in the following experiments.

To establish sublytic C5b-9-induced podocyte injury, normal human serum (NHS, complement source), obtained from healthy volunteers in Weifang Yidu Central Hospital, was stimulated with zymosan to form the C5b-9 membrane attack complex. The method as described by Ishikawa *et al* (25) was used in the present study. A total of $1x10^7$ differentiated podocytes were inoculated with different concentrations (2, 4, 6, 8, 10 and 12%) of zymosan-activated serum (ZAS) for 6 h. Heat-inactivated human serum treated was used as a control. Written informed consent was signed by all participants in the study.

Lactate dehydrogenase (LDH) detection. The concentrations of LDH were used to detect podocyte damage induced by the C5b-9 membrane attack complex (16). After $1x10^6$ podocytes were treated with ZAS, the medium supernatant was collected and the released LDH was tested using Quantitative Lactate Dehydrogenase Assay Kits (Sigma-Aldrich; Merck KGaA) according to the manufacturer's instructions. Cytotoxicity=(experimental LDH release values-background values)/(maximum LDH release values-background values) x100%

Immunofluorescence assay. A total of $1x10^4$ podocytes were fixed into 4% paraformaldehyde for 30 min at room temperature and permeabilized with 0.2% Triton X-100 for 15 min at room temperature. After blocking with 5% BSA (Thermo Fisher Scientific, Inc.) for 1 h at room temperature, the cells were cultured with primary antibody anti-C5b-9 (1:100; cat. no. #ab55811; Abcam), anti-LC3 (1:100; cat. no. #ab192890; Abcam), anti-p62 (1:100; cat. no. #ab109012; Abcam) at 4˚C overnight. On the second day, the cells were incubated with Fluorescein-AffiniPure goat anti-rabbit IgG (1:200; cat. no. #ab150077; Abcam) for 1 h at room temperature. The nuclei were counterstained with 49,69-diamidino-2-phenylindole hydrochloride (DAPI) for 15 min at 37˚C in the dark. The fluorescence intensity image was acquired through a confocal microscope (Zeiss AG).

Western blotting. Podocytes' total protein was extracted using a lysis buffer [0.1% Triton X-100, 50 mM Tris (pH 7.0), 100 Mm NaCl, 1 mM EDTA, 1 mM PMSF] and protease inhibitor cocktail (Sigma-Aldrich; Merck KGaA). The total protein in the supernatant was quantified using a BCA Protein Assay kit (cat. no. 23235; Pierce; Thermo Fisher Scientific, Inc.). Total protein (25 μg loaded per lane) was separated by 10% SDS-PAGE and transferred onto polyvinylidene difluoride membranes (Sigma-Aldrich; Merck KGaA). After blocking with 5% free-fat milk for 1 h at room temperature, the membranes were incubated with the following primary antibodies: Rabbit anti-TRPC6 (1:1,000; cat. no. #ab105845; Abcam); rabbit anti-LC3B (1:1,000; cat. no. #ab192890; Abcam); rabbit anti-p62 (1:10,000; cat. no. #ab109012; Abcam); rabbit anti-p-ERK (1:1,000; cat. no. #ab201015; Abcam); rabbit anti-t-ERK (1:5,000; cat. no. #ab184699; Abcam); and rabbit anti-GAPDH (1:2,500; cat. no. #ab9485; Abcam) antibody at 4˚C overnight. Following primary incubation, the membranes were incubated with HRP-conjugated goat anti-rabbit IgG (1:2,000, Abcam # ab6721) for 2 h at room temperature. Protein bands were visualized using an enhanced chemiluminescence detection system (MilliporeSigma) and densitometry quantitative analysis was carried out using Image J software version 1.46r (National Institutes of Health).

Cell transfection and treatment. The TRPC6 small interfering (si)RNA (si-TRPC6; sense, 5'-ATTGATCCTGGATCTAGA GTG-3) and negative control siNC (sense, 5'-UUCUCCGAA CGUGUCACGUTT-3') were synthesized by Guangzhou RiboBio Co., Ltd. When reaching 7-80% confluence, cells were transfected with 50 nM si-TRPC6/si-NC using Lipofectamine® 3000 Transfection Reagent (Invitrogen; Thermo Fisher Scientific, Inc.) at 37˚C, and 48 h later, transfected cells were used for further experimentation.

After transfection with si-TRPC6, the cells were treated with ERK1/2 activator [12-O-tetradecanoylphorbol-13-acetate (TPA)] for 12 h at 37˚C to activate ERK1/2 in podocytes.

Reverse transcription-quantitative polymerase chain reaction (RT-qPCR). Podocytes' total RNA was harvested using Trizol™ (Invitrogen; Thermo Fisher Scientific, Inc.), according to the manufacturer's protocol. Total RNA was reverse-transcribed into cDNA using TaqMan Reverse Transcription Kit (Takara Bio, Inc.), according to the manufacturer's protocol. qPCR was performed using the SYBR Green PCR kit (Thermo Fisher Scientific, Inc.), according to the manufacturer's protocol and analyzed using the ABI Prism 7500 Software version 2.0.6 (Thermo Fisher Scientific, Inc.). PCR amplification conditions were: 95˚C for 10 min, followed by 40 cycles of denaturation at 95˚C for 15 sec, 60˚C for 20 sec and 72˚C for 30 sec. The following primer pairs were used for qPCR: TRPC6 forward, 5'-GTTAACTGCGATGATCAATAGTT-3' and reverse, 5'-GACTTGGTACAAGATTGAAGG-3'; GAPDH forward, 5'-CTGCCCAGAACATCATCC-3' and reverse, 5'-CTCAGA TGCCTGCTTCAC-3'. The RNA expression level of TRPC6 was quantified using the $2^{-\Delta\Delta Cq}$ method (26) and normalized to the internal reference gene GAPDH.

Phalloidin staining. Sublytic C5b-9 treated podocytes were fixed into 4% paraformaldehyde for 40 min at room temperature. Whereafter, the cells were permeabilized in 0.5% Triton X-100 for 10 min at room temperature. Subsequently, podocytes were incubated in 200 μl rhodamine phalloidin reagent (Sigma-Aldrich; Merck KGaA) for 30 min in the dark at room temperature. And DAPI was applied to stain the nucleus. The images were observed under a confocal microscope (Zeiss AG).

Cell Counting Kit-8 (CCK-8) assay. The viability of podocytes transfected with siTRPC6 was detected using a CCK-8 (Dojindo Laboratories, Inc.). In brief, $5x10^3$ cells/well were seeded into a 96-well plate. After incubating, 10 μl CCK-8 was added to the medium for 2 h. The absorbance values were tested in a microplate reader (Guangzhou RiboBio Co., Ltd.) at 450 nm.

Flow cytometry analysis. The cell apoptosis rate of damaged podocytes was examined through double staining with Annexin V-FITC Apoptosis Detection kit (cat. no. #C1062M; Beyotime Institute of Biotechnology). Cells were collected and cultured with 5 μl annexin V-FITC for 15 min at room temperature, and continually cultured with 10 μl PI for 10 min in the dark at room temperature. Subsequently, cell apoptosis was analyzed through the CytoFLEX (Beckman Coulter, Inc.).

Transmission electron microscopy (TEM). TEM was performed according to a previous method (18). Podocytes were fixed first in 2.5% glutaraldehyde for 1 h at 4˚C and then in 1% OsO_4 for 1 h at room temperature, and dehydrated using 30, 50, 70, 80, 90, 95 and 100% ethanol in series. Cells were stained with 2% uranyl acetate for 20 min at room temperature and lead citrate for 5 min at room temperature. After drying, the autophagosomes were visualized using an Hitachi 7500 transmission electron microscope aperture grid with 100 μm at 80 kV, x10K in HC-1 mode (Hitachi, Ltd.).

Lysosomal enzyme activity detection. The effect of TRPC6 on the lysosomal fusion stage of autophagy was evaluated through the lysosomal enzyme activity. The lysosomal enzyme activity was detected using Cathepsin B Activity Assay kit and Cathepsin L Activity Assay kit (cat. nos. #MAK387 and #CBA023; Sigma-Aldrich; Merck KGaA) according to the manufacturer's instructions. A total of $1x10^5$ podocytes treated with 10 μM Chloroquine (CQ) for 48 h was used as positive control.

Statistical analysis. Data are presented as means ± standard deviation. Statistical analysis was carried out using GraphPad Prism 8.3 (Dotmatics). The Student's t-test was used to compare the difference between the two groups, whilst one-way ANOVA followed by Bonferroni post hoc test was used to analyze the difference between >2 groups. All experiments were repeated three times. $P < 0.05$ was considered to indicate a statistically significant difference.

Results

The expression of TRPC6 is increased in sublytic C5b-9-induced podocytes. To investigate the specific damage mechanism of C5b-9 to podocytes, ZAS was used to establish the podocyte
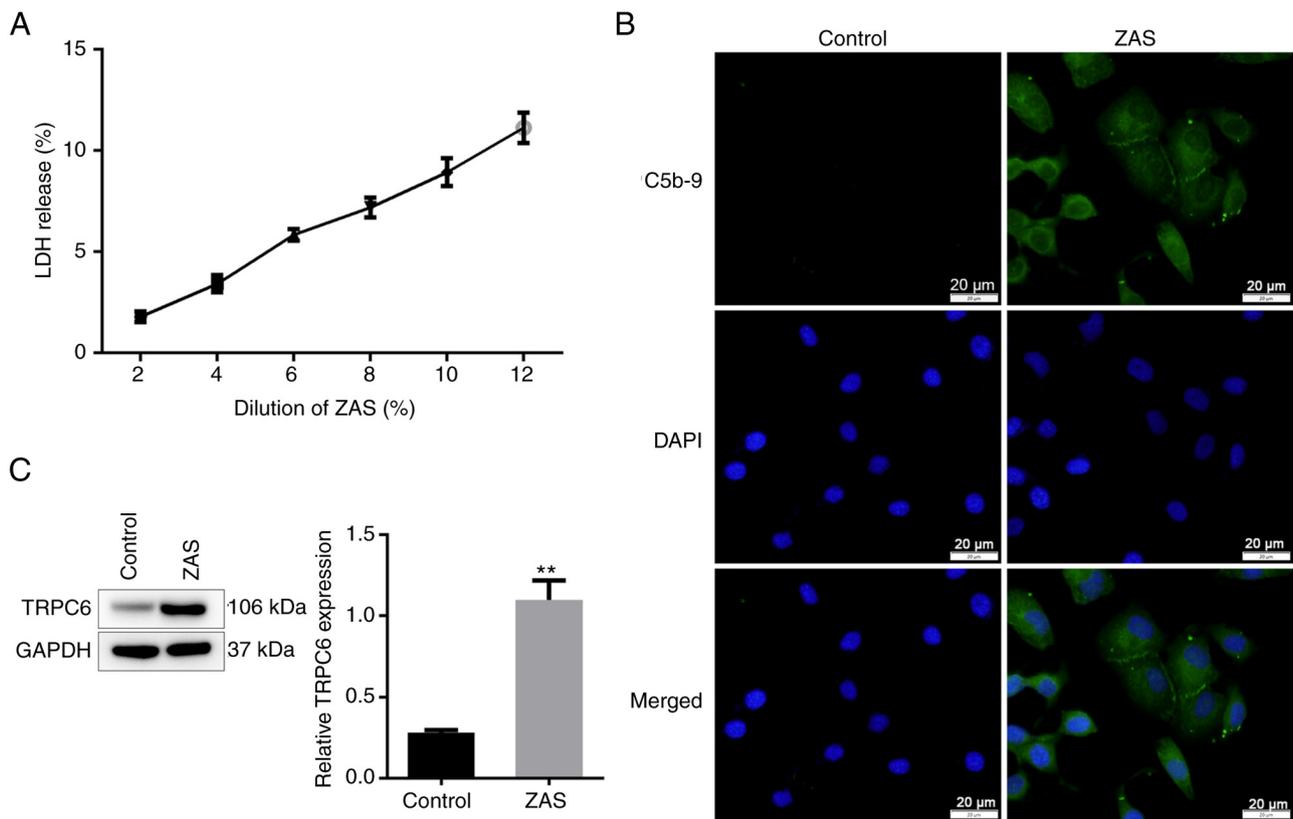
Figure 1. Sublytic C5b-9 causes damage to podocytes exposed in zymosan-activated serum. (A) The effect of sublytic C5b-9 on podocytes' cytotoxicity was detected by LDH release through an LDH detection kit. (B) An immunofluorescence assay was applied to test the accumulation of sublytic C5b-9 in podocytes. Scale bar, 20 μm. (C) The expression of TRPC6 was examined by western blotting. Bar graphs showed the relative intensity quantification of the TRPC6/GAPDH ratio. **P<0.01. LDH, lactate dehydrogenase.

injury model. The LDH release increased following treatment with ZAS in a dose-dependent manner, indicating damage to the podocytes' membranes. The LDH level was <10% when ZAS was at 10% dilution and this condition was chosen to establish a C5b-9-induced podocytes injury model in subsequent experiments (Fig. 1A). To investigate whether sublytic C5b-9 accumulated in podocytes, an immunofluorescent assay was performed to evaluate the level of C5b-9. Compared with the cells treated with heat-inactivated human serum, C5b-9 was successfully deposited in podocytes treated with ZAS (Fig. 1B). Subsequently, the results of western blotting showed that the expression of TRPC6 was enhanced in sublytic C5b-9-induced podocytes (Fig. 1C).

Knockdown of TRPC6 attenuates the damage of podocytes induced by C5b-9. To determine whether TRPC6 serves a role in sublytic C5b-9-induced podocyte damage, TRPC6 was knocked down through siTRPC6 transfection in podocytes before sublytic C5b-9 induction. As shown in Fig. 2A and B, the mRNA and protein levels of TRPC6 were significantly decreased in podocytes transfected with siTRPC6. Moreover, transfection of siTRPC6 decreased the expression of TRPC6 in sublytic C5b-9-induced podocytes, compared with that in C5b-9-induced podocytes transfected with siNC (Fig. 2C and D). Subsequently, the viability of podocytes was detected using CCK-8 assay. C5b-9 decreased the viability of podocytes and the knockdown of TRPC6 reversed the reduced viability in sublytic C5b-9-induced podocytes

(Fig. 2E). Moreover, the results of phalloidin staining showed that sublytic C5b-9 visibly destroyed actin stress fiber and the loss of actin stress fiber was relieved by TRPC6 inhibition in sublytic C5b-9-induced podocytes (Fig. 2F). In addition, flow cytometry analysis was applied to examine the effect of TRPC6 on the apoptosis of sublytic C5b-9-induced podocytes and the result revealed that the apoptosis rate was 25.63% in the C5b-9 group, whilst it was reduced to 9.68% in C5b-9 + siTRPC6 group (Fig. 2G). Together, the results suggested that TRPC6 knockdown inhibited sublytic C5b-9-induced podocyte injury and cell apoptosis.

TRPC6 inhibition promotes the autophagy of C5b-9-induced podocytes. Subsequently, it was evaluated whether TRPC6 regulates autophagy in sublytic C5b-9-induced podocytes. As shown in Fig. 3A, sublytic C5b-9 improved the level of LC3-II and the knockdown of TRPC6 suppressed LC3-II turnover mediated by sublytic C5b-9 in podocytes. Similarly, the positive puncta of LC3 raised in sublytic C5b-9-treated podocytes, whereas it weakened in sublytic C5b-9-treated podocytes transfected with siTRPC6 (Fig. 3B). The effect of TRPC6 on the autophagy of sublytic C5b-9-treated podocytes was also evaluated through fluorescence staining of p62. After podocytes were exposed to ZAS, the positive staining of p62 was increased (Fig. 3B), which indicated that sublytic C5b-9 suppressed the autophagy of podocytes. Knockdown of TRPC6 partially bated the level of p62 in sublytic C5b-9-treated podocytes (Fig. 3B). In addition, autophagic vesicles were observed
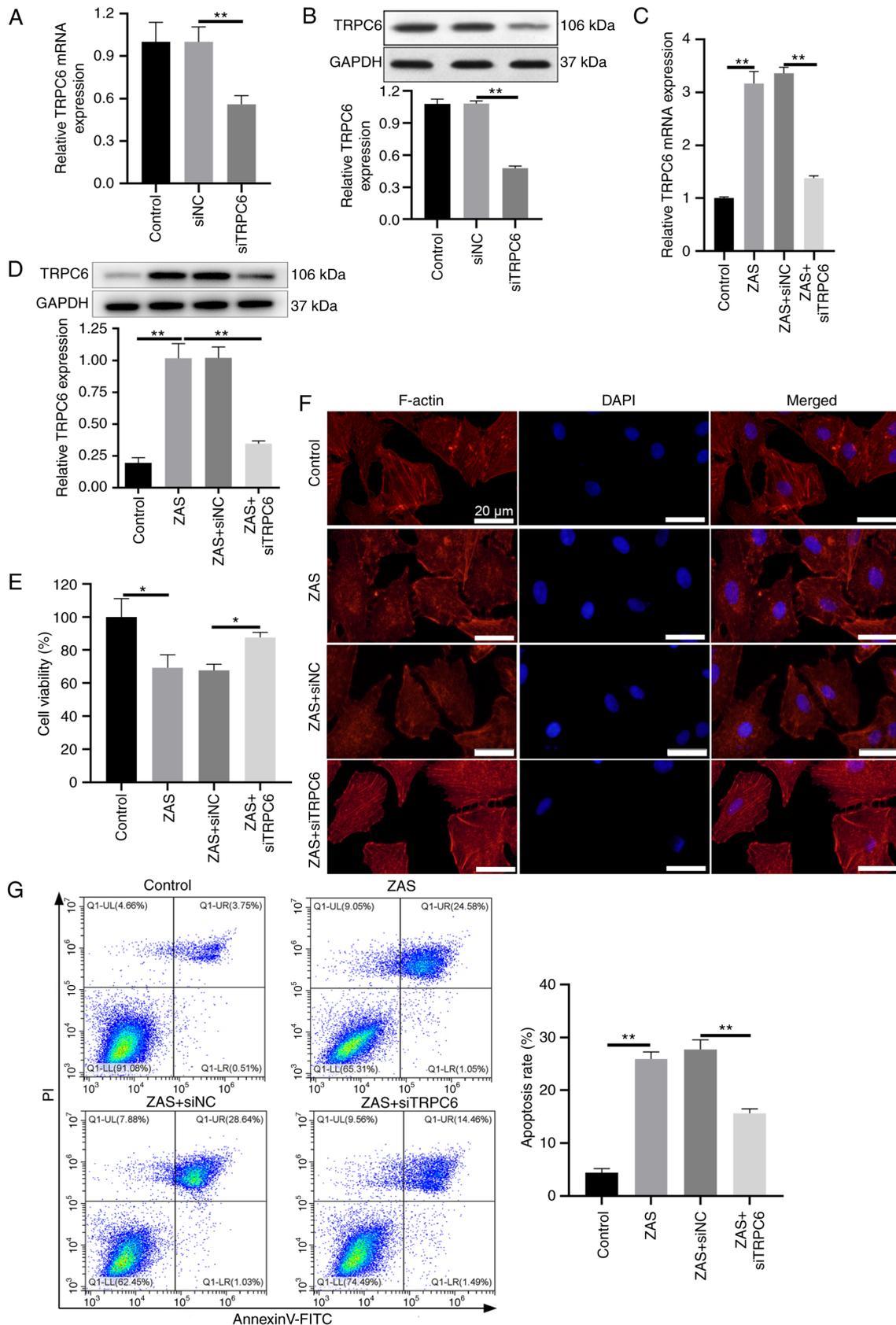
Figure 2. Knockdown of TRPC6 suppresses the injury of podocytes induced by C5b-9. (A) The RNA and (B) protein expression levels of TRPC6 were analyzed in podocytes through reverse transcription-quantitative PCR and western blotting, respectively. Bar graphs showed the relative intensity quantification of the TRPC6/GAPDH ratio. (C) The RNA and (D) protein expression levels of TRPC6 were analyzed in podocytes exposed to ZAS through reverse transcription-quantitative PCR and western blotting, respectively. Bar graphs showed the relative intensity quantification of the TRPC6/GAPDH ratio. (E) The cell viability of podocytes transfected with TRPC6 was detected using the Cell Counting Kit-8 assay. (F) Destruction of actin filaments in sublytic C5b-9-induced podocytes transfected with TRPC6 was analyzed by phalloidin staining. Scale bar, 20 μm. (G) The apoptosis rate of podocytes treated with sublytic C5b-9 and/or small-interfering RNA targeting TRPC6 was tested using flow cytometry analysis. $^*P<0.05$ and $^{**}P<0.01$. TRPC6, transient receptor potential 6; ZAS, zymosan activated serum; siTRPC6, small interfering RNA targeting TRPC6; siNC, small interfering RNA negative control.
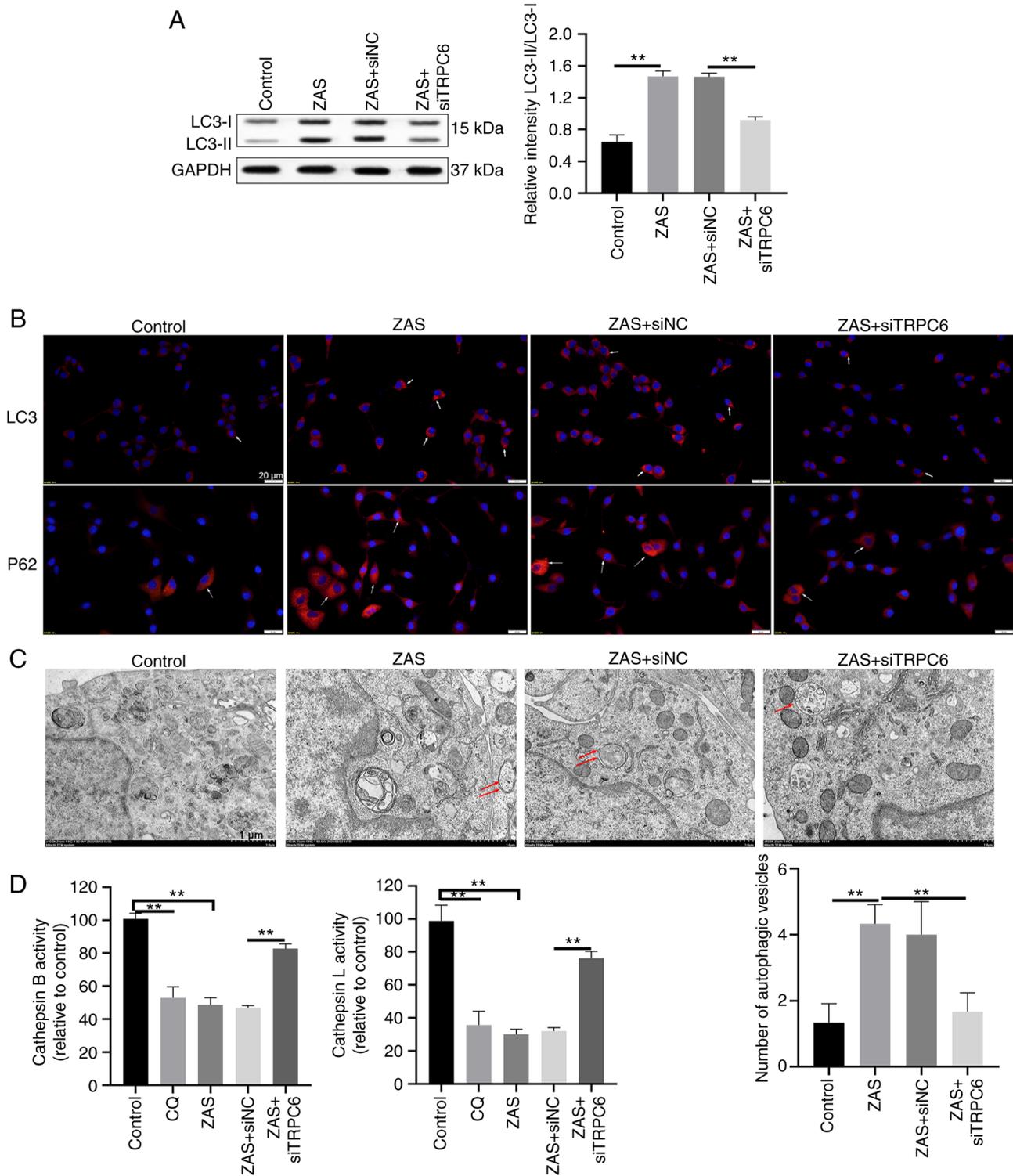
Figure 3. TRPC6 inhibition promotes the autophagy of podocytes treated with sublytic C5b-9. (A) The expression of LC3-I and LC3-II proteins was analyzed using western blotting. Bar graphs showed the relative intensity quantification of the LC3-I/LC3-II ratio. (B) Podocytes were treated with sublytic C5b-9 and/or siTRPC6, and fluorescence images of LC3 and p62 were captured through immunofluorescence assay. Scale bar, 20 μm. (C) Podocytes were treated with sublytic C5b-9 and/or siTRPC6, and the ultrastructure of autophagic vesicles was observed by transmission electron microscopy. Scale bar, 10 μm. (D) Lysosomal proteolytic enzyme (cathepsin B and cathepsin L) activity was tested using the respective kits. **P<0.01. TRPC6, transient receptor potential 6; ZAS, zymosan activated serum; siTRPC6, small interfering RNA targeting TRPC6; siNC, small interfering RNA negative control; CQ, chloroquine.

under TEM in sublytic C5b-9-treated podocytes. The number of autophagosomes and damaged lysosomes increased in the C5b-9 group (Fig. 3C). The number of autophagy-lysosomes raised in the C5b-9 + siTRPC6 group, compared with that in

the C5b-9 and C5b-9 + siNC groups (Fig. 3C). CQ was shown to inhibit the fusion between autophagosome and lysosome and the degradation of lysosome protein by increasing the pH value of lysosome (27). Subsequently, lysosome enzyme activity in

podocytes was evaluated. The activity of both cathepsin B and cathepsin L was decreased in sublytic C5b-9-treated podocytes and chloroquine-treated podocytes, while the knockdown of TRPC6 reversed the effect on the activity of cathepsin B and cathepsin L in sublytic C5b-9-treated podocytes (Fig. 3D). The above results indicated that knockdown of TRPC6 facilitated autophagy in sublytic C5b-9-induced podocytes.

Knockdown of TRPC6 protects sublytic C5b-9-induced podocytes via inhibiting phosphorylation of ERK1/2. Activated ERK was found in sublytic C5b-9-induced podocytes (23) and the regulatory relationship between TRPC6 and ERK1/2 (MAPK3/1) was predicted using the STRING database (Fig. 4A). Subsequently, whether TRPC6 regulated the activation of ERK1/2 in sublytic C5b-9-induced podocytes was elucidated. It was revealed through western blot analysis that sublytic C5b-9 enhanced the phosphorylation level of ERK1/2 and TRPC6 knockdown decreased the level of p-ERK1/2 (Fig. 4B). Subsequently, TPA was used to treat siTRPC6 transfected podocytes and CCK-8 assay and flow cytometry analysis showed that TPA inhibited viability and increased the apoptosis of sublytic C5b-9-induced podocytes (Fig. 4C and D). The addition of TPA partly reversed the protective effect of TRPC6 knockdown on sublytic C5b-9-induced podocytes (Fig. 4C and D). To deeply investigate the effect of ERK1/2 on the autophagy of TRPC6 inhibitor transfected and sublytic C5b-9-induced podocytes, the protein levels of LC3 and p62 were assessed. It was presented that TPA improved LC3-II and p62 levels in sublytic C5b-9-induced podocytes (Fig. 4E). Likewise, compared with those in the ZAS + siTRPC6 group, the levels of LC3-II and p62 were elevated in ZAS + siTRPC6+TPA group (Fig. 4E). TPA also partially reversed the effect of TRPC6 on the activity of cathepsin B and cathepsin L (Fig. 4F). All of these findings illustrated that TRPC6 regulated autophagy by activating phosphorylation ERK1/2 in sublytic C5b-9-induced podocytes.

Discussion

MN accounts for 25-40% of nephrotic syndromes and IMN accounts for about two-thirds of MN (2). The ineffective treatment of patients with IMN results in chronic urinary protein, hypoproteinemia and metabolic disorders, which eventually lead to end-stage renal failure (2). Therefore, it is very important to further study the pathogenesis of IMN and to find effective therapeutic targets and methods. A previous study reported that the level of the C5b-9 membrane attack complex, a product of complement activation, was higher than that of the control in the urine of MN animal model (28). The sublytic C5b-9 can directly cause podocyte injury (29). The podocytes, basement membrane and endodermal cells form the glomerular filtration barrier. The damage of podocytes can lead to proteinuria (5). So podocyte damage is the direct cause of renal glomerular disease. In the current study, normal human serum was stimulated with zymosan to obtain a sublytic C5b-9 complex and established a sublytic C5b-9-induced podocyte injury model. The deposition of C5b-9 was observed in the podocyte injury model. Meanwhile, cell viability was reduced and the apoptosis rate was raised in sublytic C5b-9-induced podocytes. These results were consistent with the finding of

Zheng *et al* (30) which reported that sublytic C5b-9 induced podocyte injury. In addition, F-actin is the main support of the foot process structure of podocytes. Sublytic C5b-9 could dissolve F-actin and adhesion plaque complexes (29) and the present research verified that F-actin was detected in sublytic C5b-9-induced podocytes.

TRPC6 participates in several physiological and pathological processes. For example, appropriate mechanical force activated TRPC6 to regulate periodontal tissue reconstruction (31). TRPC6 promoted LPS-induced inflammatory response in bronchial epithelial cells (32). TRPC6 interacts with podocin, nephrin, actin-4 and CD2-associated proteins to maintain the structure and function of glomerular podocytes (19). Enhanced expression of TRPC6 was found in human urinary protein nephropathy such as IMN (19), while sublytic C5b-9 mediated elevated expression of TRPC6 in cultured podocytes *in vitro* (20). The combination of PLA2R on podocytes and anti-PLA2R antibodies activated the TRPC6 channel and increased the expression of TRPC6, resulting in the structural and functional impairment of podocytes (33). In the present study, increased expression of TRPC6 was detected in sublytic C5b-9-induced podocytes. After siTRPC6 transfection in sublytic C5b-9-induced podocytes, the cell damage was weakened.

Autophagy is a biological process of degradation of cytoplasmic macromolecules and organelles in capsular vesicles (27). Cell removes cellular wastes and carries out structural reconstruction to maintain protein metabolism balance and cellular environment stability through autophagy (27). Podocytes, glomerular endothelial cells and renal tubular epithelial cells all maintain basal autophagy to keep the normal physiological functions of the cells (34,35). In lupus nephritis, autophagy exhibited a cell-protective effect on antibody-induced podocyte damage (36). The synergistic action of autophagy in epithelial and podocyte cells inhibits diabetic glomerulosclerosis (37). A previous study found that in sublytic C5b-9-treated podocytes, the number of autophagosomes was increased but the number of autophagic lysosomes was decreased and the lysosomes were destroyed, which indicated that sublytic C5b-9 inhibited the autophagy process (16). In addition, previous research reported that TRPC6 promoted oxidative stress-mediated renal tubular epithelial cell apoptosis by inhibiting autophagy and suppressing autophagy in Ang-II-induced podocyte apoptosis (22,38). Knockdown of TRPC6 improved renal ischemia/reperfusion by enhancing autophagy (18). The results of the present study showed that the knockdown of TRPC6 could weaken podocyte apoptosis by facilitating the progress of autophagy.

Subsequently, the present authors deeply investigated the mechanism of TRPC6 in the regulation autophagy of sublytic C5b-9 treated podocytes. By using the STRING database, it was predicted that ERK1/2 and TRPC6 had a regulatory relationship. Moreover, the result of the western blot assay revealed that the level of phosphorylation of ERK1/2 was elevated in sublytic C5b-9 treated podocytes and reduced due to the transfection of siTRPC6. The present findings were consistent with the discovery of Zheng *et al* (30) that sublytic C5b-9 promoted podocyte injury by activating the phosphorylation of ERK1/2. TRPC6-increased intracellular Ca^{2+} could
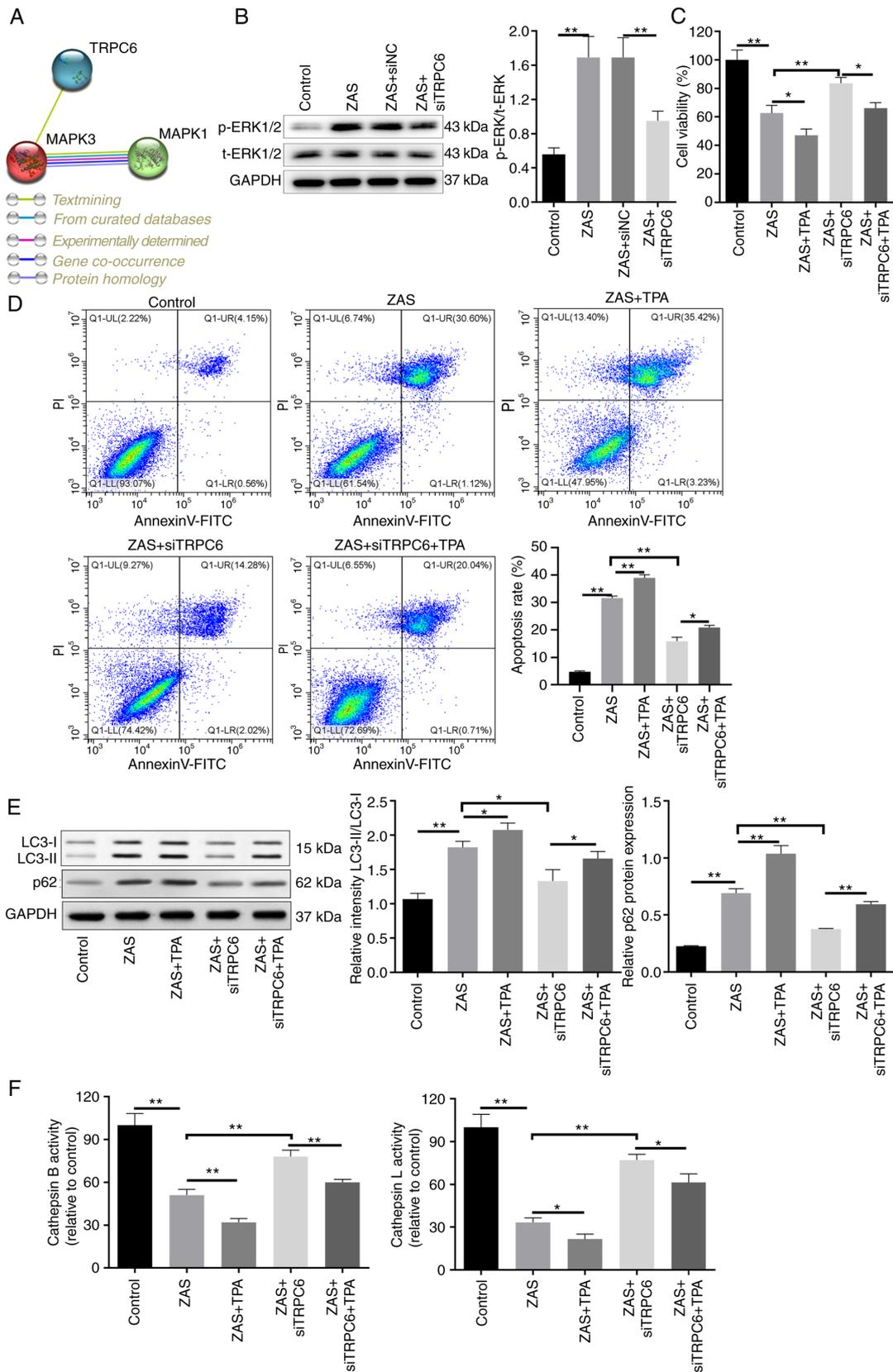
Figure 4. TRPC6 knockout in sublytic C5b-9-induced podocytes affects the regulation of the phosphorylation of ERK1/2. (A) The regulatory relationship between TRPC6 and ERK1/2 (MAPK3/1) was predicted using the STRING database. (B) The phosphorylation of ERK1/2 was analyzed through western blotting in podocytes treated with sublytic C5b-9 and/or siTRPC6. Bar graphs showed the relative intensity quantification of phosphorylated ERK1/2/total-ERK. (C) Cell Counting Kit-8 and (D) flow cytometry analysis were carried out to analyze the viability and apoptosis of podocytes treated with sublytic C5b-9 and/or siTRPC6 and/or TPA, respectively. (E) The levels of autophagy relative proteins (LC3 and p62) were inspected via western blot assay. Bar graphs showed the relative intensity quantification of LC3-I/LC3-II and p62/GAPDH ratios. (F) Lysosomal proteolytic enzyme (cathepsin B and cathepsin L) activity was tested in podocytes treated with sublytic C5b-9 and/or siTRPC6 and/or TPA with respective kits. *P<0.05 and **P<0.01. TRPC6, transient receptor potential 6; ZAS, zymosan activated serum; siTRPC6, small interfering RNA targeting TRPC6; siNC, small interfering RNA negative control; p-, phosphorylated; t-, total; TPA, 12-O-tetradecanoylphorbol-13-acetate.

activate ERK1/2 phosphorylation to promote inflammation in bronchial epithelial cells (32) and TRPC6 interacted with ERK1/2 (39). In addition, it was also shown that apelin blocked the autophagy of podocytes in diabetic nephropathy by activating ERK1/2 (24). In the present study, an ERK1/2 activator was applied to activate the phosphorylation of ERK1/2 in siTRPC6 transfected podocytes induced by sublytic C5b-9. The results demonstrated that the ERK1/2 activation partially reversed the effect of TRPC6 on sublytic C5b-9-treated podocytes. However, whether the specific regulatory mechanism between TRPC6 and ERK1/2 was directly or indirectly acting through the involvement of other molecules in podocytes needs further investigation.

The present data revealed that sublytic C5b-9 induced the injury of podocytes as well as knockdown of TRPC6 weakened the injury of sublytic C5b-9-induced podocytes. Furthermore, the knockdown of TRPC6 promoted the progression of autophagy by inhibiting the phosphorylation of ERK1/2 in sublytic C5b-9-induced podocytes. The present study provided important evidence for the regulatory roles of TRPC6 on autophagy in sublytic C5b-9-induced podocytes which might provide a new basal mechanism for the treatment of IMN.

Acknowledgements

Availability of data and materials

The datasets used and/or analyzed during the current study are available from the corresponding author on reasonable request.

Authors' contributions

YYL and YFF conceived and designed the project, and wrote the paper. JL acquired and analyzed the data. YFF modified the manuscript. YYL and YFF confirm the authenticity of all the raw data. All authors read and approved the final version of the manuscript.

Ethics approval and consent to participate

This research was approved by the Ethical Committee of Weifang Yidu Central Hospital (approval no. 2017-032 and obeyed the principles of the Declaration of Helsinki. Written informed consent was signed by all participants in the study.

Patient consent for publication

Not applicable.

Competing interests

The authors declare that they have no competing interests.

References

1. Keri KC, Blumenthal S, Kulkarni V, Beck L and Chongkrairatanakul T: Primary membranous nephropathy: Comprehensive review and historical perspective. Postgrad Med J 95: 23-31, 2019.
2. Safar-Boueri L, Piya A, Beck LH Jr and Ayalon R: Membranous nephropathy: Diagnosis, treatment, and monitoring in the post-PLA2R era. Pediatr Nephrol 36: 19-30, 2021.
3. Liu W, Gao C, Liu Z, Dai H, Feng Z, Dong Z, Zheng Y, Gao Y, Tian X and Liu B: Idiopathic membranous nephropathy: Glomerular pathological pattern caused by extrarenal immunity activity. Front Immunol 11: 1846, 2020.
4. Ma H, Sandor DG and Beck LH Jr: The role of complement in membranous nephropathy. Semin Nephrol 33: 531-542, 2013.
5. Nagata M: Podocyte injury and its consequences. Kidney Int 89: 1221-1230, 2016.
6. Galindo-Izquierdo M and Pablos Alvarez JL: Complement as a therapeutic target in systemic autoimmune diseases. Cells 10: 148, 2021.
7. Yang P, Skiba NP, Tewkesbury GM, Treboschi VM, Baciu P and Jaffe GJ: Complement-mediated regulation of apolipoprotein E in cultured human RPE cells. Invest Ophthalmol Vis Sci 58: 3073-3085, 2017.
8. Fishelson Z and Kirschfink M: Complement C5b-9 and Cancer: Mechanisms of cell damage, cancer counteractions, and approaches for intervention. Front Immunol 10: 752, 2019.
9. Takano T, Elimam H and Cybulsky AV: Complement-mediated cellular injury. Semin Nephrol 33: 586-601, 2013.
10. Bateman RM, Sharpe MD, Jagger JE, Ellis CG, Solé-Violán J, López-Rodríguez M, Herrera-Ramos E, Ruíz-Hernández J, Borderías L, Horcajada J, et al: 36th International symposium on intensive care and emergency medicine: Brussels, Belgium. 15-18 March 2016. Crit Care 20 (Suppl 2): S94, 2016.
11. Tan Y and Zhao MH: Complement in glomerular diseases. Nephrology (Carlton) 23 (Suppl 4): S11-S15, 2018.
12. Xie H, Yang L, Yang Y, Jiang W, Wang X, Huang M, Zhang J and Zhu Q: C5b-9 membrane attack complex activated NLRP3 inflammasome mediates renal tubular immune injury in trichloroethylene sensitized mice. Ecotoxicol Environ Saf 208: 111439, 2021.
13. Wang X, Liu J, Tian R, Zheng B, Li C, Huang L, Lu Z, Zhang J, Mao W, Liu B, et al: Sanqi oral solution mitigates proteinuria in rat passive heymann nephritis and blocks podocyte apoptosis via Nrf2/HO-1 Pathway. Front Pharmacol 12: 727874, 2021.
14. Zhou XJ, Klionsky DJ and Zhang H: Podocytes and autophagy: A potential therapeutic target in lupus nephritis. Autophagy 15: 908-912, 2019.
15. Yoshibayashi M, Kume S, Yasuda-Yamahara M, Yamahara K, Takeda N, Osawa N, Chin-Kanasaki M, Nakae Y, Yokoi H, Mukoyama M, et al: Protective role of podocyte autophagy against glomerular endothelial dysfunction in diabetes. Biochem Biophys Res Commun 525: 319-325, 2020.
16. Liu WJ, Li ZH, Chen XC, Zhao XL, Zhong Z, Yang C, Wu HL, An N, Li WY and Liu HF: Blockage of the lysosome-dependent autophagic pathway contributes to complement membrane attack complex-induced podocyte injury in idiopathic membranous nephropathy. Sci Rep 7: 8643, 2017.
17. Liu X, Yao X and Tsang SY: Post-Translational modification and natural mutation of TRPC Channels. Cells 9: 135, 2020.
18. Hou X, Huang M, Zeng X, Zhang Y, Sun A, Wu Q, Zhu L, Zhao H and Liao Y: The Role of TRPC6 in renal ischemia/reperfusion and cellular hypoxia/reoxygenation injuries. Front Mol Biosci 8: 698975, 2021.
19. Dryer SE, Roshanravan H and Kim EY: TRPC channels: Regulation, dysregulation and contributions to chronic kidney disease. Biochim Biophys Acta Mol Basis Dis 1865: 1041-1066, 2019.
20. Moller CC, Wei C, Altintas MM, Li J, Greka A, Ohse T, Pippin JW, Rastaldi MP, Wawersik S, Schiavi S, et al: Induction of TRPC6 channel in acquired forms of proteinuric kidney disease. J Am Soc Nephrol 18: 29-36, 2007.
21. Yu S and Yu L: Dexamethasone resisted podocyte injury via stabilizing TRPC6 expression and distribution. Evid Based Complement Alternat Med 2012: 652059, 2012.
22. Shengyou Y and Li Y: The effects of siRNA-silenced TRPC6 on podocyte autophagy and apoptosis induced by AngII. J Renin Angiotensin Aldosterone Syst 16: 1266-1273, 2015.

23. Zhang MH, Fan JM, Xie XS, Deng YY, Chen YP, Zhen R, Li J, Cheng Y and Wen J: Ginsenoside-Rg1 protects podocytes from complement mediated injury. J Ethnopharmacol 137: 99-107, 2011.
24. Liu Y, Zhang J, Wang Y and Zeng X: Apelin involved in progression of diabetic nephropathy by inhibiting autophagy in podocytes. Cell Death Dis 8: e3006, 2017.
25. Ishikawa S, Tsukada H and Bhattacharya J: Soluble complex of complement increases hydraulic conductivity in single microvessels of rat lung. J Clin Invest 91: 103-109, 1993.
26. Schmittgen TD and Livak KJ: Analyzing Real-time PCR data by the comparative C(T) method. Nat Protoc 3: 1101-1108, 2008.
27. Pasquier B: Autophagy inhibitors. Cell Mol Life Sci 73: 985-1001, 2016.
28. Jefferson JA, Pippin JW and Shankland SJ: Experimental models of membranous nephropathy. Drug Discov Today Dis Models 7: 27-33, 2010.
29. Papagianni AA, Alexopoulos E, Leontsini M and Papadimitriou M: C5b-9 and adhesion molecules in human idiopathic membranous nephropathy. Nephrol Dial Transplant 17: 57-63, 2002.
30. Zheng R, Deng Y, Chen Y, Fan J, Zhang M, Zhong Y, Zhu R and Wang L: Astragaloside IV attenuates complement membranous attack complex induced podocyte injury through the MAPK pathway. Phytother Res 26: 892-898, 2012.
31. Wang L, Liang H, Sun B, Mi J, Tong X, Wang Y, Chen M, Yu L, Pan J, Liu S, *et al*: Role of TRPC6 in periodontal tissue reconstruction mediated by appropriate stress. Stem Cell Res Ther 13: 401, 2022.
32. Zhou LF, Chen QZ, Yang CT, Fu ZD, Zhao ST, Chen Y, Li SN, Liao L, Zhou YB, Huang JR and Li JH: TRPC6 contributes to LPS-induced inflammation through ERK1/2 and p38 pathways in bronchial epithelial cells. Am J Physiol Cell Physiol 314: C278-C288, 2018.
33. Putta P, Smith AH, Chaudhuri P, Guardia-Wolff R, Rosenbaum MA and Graham LM: Activation of the cytosolic calcium-independent phospholipase A_2 β isoform contributes to TRPC6 externalization via release of arachidonic acid. J Biol Chem 297: 101180, 2021.
34. Hartleben B, Godel M, Meyer-Schwesinger C, Liu S, Ulrich T, Kobler S, Wiech T, Grahammer F, Arnold SJ, Lindenmeyer MT, *et al*: Autophagy influences glomerular disease susceptibility and maintains podocyte homeostasis in aging mice. J Clin Invest 120: 1084-1096, 2010.
35. Fang L, Zhou Y, Cao H, Wen P, Jiang L, He W, Dai C and Yang J: Autophagy attenuates diabetic glomerular damage through protection of hyperglycemia-induced podocyte injury. PLoS One 8: e60546, 2013.
36. Qi YY, Zhou XJ, Cheng FJ, Hou P, Ren YL, Wang SX, Zhao MH, Yang L, Martinez J and Zhang H: Increased autophagy is cytoprotective against podocyte injury induced by antibody and interferon-α in lupus nephritis. Ann Rheum Dis 77: 1799-1809, 2018.
37. Lenoir O, Jasiek M, Henique C, Guyonnet L, Hartleben B, Bork T, Chipont A, Flosseau K, Bensaada I, Schmitt A, *et al*: Endothelial cell and podocyte autophagy synergistically protect from diabetes-induced glomerulosclerosis. Autophagy 11: 1130-1145, 2015.
38. Hou X, Xiao H, Zhang Y, Zeng X, Huang M, Chen X, Birnbaumer L and Liao Y: Transient receptor potential channel 6 knockdown prevents apoptosis of renal tubular epithelial cells upon oxidative stress via autophagy activation. Cell Death Dis 9: 1015, 2018.
39. Farmer LK, Rollason R, Whitcomb DJ, Ni L, Goodliff A, Lay AC, Birnbaumer L, Heesom KJ, Xu SZ, Saleem MA and Welsh GI: TRPC6 binds to and activates calpain, independent of its channel activity, and regulates podocyte cytoskeleton, cell adhesion, and motility. J Am Soc Nephrol 30: 1910-1924, 2019.